

## Effect of catalyst pore size on styrene production rate

M. E. Zeynali

m.zeynali@ippi.ac.ir

Petrochemical Synthesis Group, Petrochemical Faculty, Iran Polymer and Petrochemical Institute (IPPI), P. O. Box: 14965/115, Tehran, Iran,

### Abstract

In this study the diffusion coefficients for reaction components were determined for unimodal and bimodal pore size distribution and assuming transitional diffusion regime using a more realistic, Stewart-Johnson, method. It was found that determination of diffusion coefficient using the average pore size results in underestimated values. A comparison was made between the effects of unimodal and bimodal pore size distribution on diffusion coefficients. The governing differential equation for a single pellet for styrene production was solved by orthogonal collocation method. The effectiveness factor which is a key parameter in reactor design was determined for the reaction in practical range of pore size. It was found that the production rate and effectiveness factor are sensitive to pore size and pore size distribution and with certain pore size distribution a considerable improvement in production rate can be achieved.

**Key words:** catalyst, diffusion coefficient, orthogonal collocation, styrene, effectiveness factor.

### Introduction

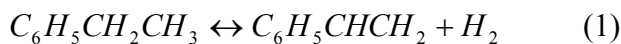
Styrene is a very important petrochemical product and its annual consumption is more than 20 mt. It is used for polystyrene production. Styrene is produced by endothermic dehydrogenation of ethylbenzene using iron oxide based catalysts at 600-650 °C and near atmospheric pressure. Three series adiabatic reactors normally are used in industrial scale. Based on the study of effect of the internal diffusion on apparent activation energy Lee believes that the internal diffusion limitation exists in the styrene synthesis reaction (1). Also reaction rate measurements using powder and pellet catalysts show that there is

internal diffusion limit in the styrene synthesis reaction (2). Therefore to increase the overall reaction rate the pore size of the catalyst should be increased. How far the diffusion coefficient can be increased as a result of increase in pore size? Is the effectiveness factor too much sensitive to pore size and pore size distribution? This is a diffusion-reaction problem and to elucidate it the effectiveness factors must be determined for the reaction in styrene synthesis for various pore sizes considering multi-component diffusion system. Apparently in a heterogeneous catalytic reaction the rate determining stage depends on the relative magnitude of diffusion rate and intrinsic reaction rate. If the intrinsic reaction rate is fast enough the diffusion rate limits the overall reaction rate. For a porous catalyst the diffusion rate is a function of pore size of the catalyst. The direct effect of pore size on diffusion coefficient and effectiveness factor has not been given quantitatively in the literature.

Nano sized pore catalyst with high efficiency has been used for styrene production [3]. Various average catalyst pore size have been used in styrene production [4,5,6]. The main objective of this study is to find the variation of production rate and effectiveness factor with pore size to obtain the limits of reaction and diffusion control in styrene synthesis process to design optimum performance catalysts and reactor.

### **Data and model equations**

Following equilibrium limited main catalytic reaction is considered in this study:



Five other reactions take place in the styrene production. These reactions involve minor products and reactants which are ignored in this study.

The reaction rate equation is as follows:

$$r_1 = k_1(p_{EB} - p_{ST}p_{H_2}/K_{EB}) \quad (2)$$

The equilibrium constant for reaction 1 is [7]:

$$K_{EB} = (T)^{0.549} \exp[-14516/T + 11.41] \quad (3)$$

The reaction rate constant can be expressed as follows:

$$k_i = \exp[A_i - (E_i/R_g T)] \quad (4)$$

Where  $A_i$  and  $E_i$  are apparent frequency factor and activation energy of reaction are given in Tab. 1 [8].

Frequency Factor $A_i$	Activation Energy $E_i$ (kJ/kgmol)
0.02	8.071X10 <sup>4</sup>

Table 1: Activation energy and frequency factor for reaction rate constant

For a spherical catalyst pellet the continuity equation for isothermal condition in terms of the partial pressure of the components is:

$$\frac{1}{r^2} \frac{d}{dr} \left( r^2 \frac{dp_m}{dr} \right) = \frac{R_g T \rho_s}{D_m} r_m \quad (5)$$

Using following dimensionless variables the continuity equation can be transformed to the dimensionless form:

$$\xi = \frac{r}{d_p / 2} \quad (6)$$

$$p_m^* = \frac{p_m}{p_{m,s}} \quad (7)$$

$$\frac{1}{\xi^2} \frac{d}{d\xi} \left( \xi^2 \frac{dp_m^*}{d\xi} \right) = \frac{d_p^2}{4} \frac{1}{D_m} \frac{R_g T \rho_s}{p_{m,s}} r_m \quad (8)$$

The boundary conditions for the above differential equation are:

$$\xi = 1, p_m^* = 1 \quad (9)$$

$$\xi = 0, \frac{dp_m^*}{d\xi} = 0 \quad (10)$$

It can be seen that with transformation the boundaries domain becomes  $[0,1]$ . This makes the calculation easier when using the roots of the Jacobi polynomials as the collocation points in  $[0,1]$  interval.

### Orthogonal collocation

The above differential equation can be solved by orthogonal collocation method. Due to symmetry of the spherical catalyst pellet the Jacobi polynomial is assumed as a trial

solution for the above differential equations. The following which satisfies the second boundary condition (Eq. 10) is the proper function as trial solution:

$$y(x^2) = y(1) + (1-x^2) \sum_{i=1}^N a_i P_{i-1}(x^2) \quad (11)$$

The equivalent choices are:

$$y(x^2) = \sum_{i=1}^N b_i P_{i-1}(x^2) = \sum_{i=1}^{N+1} d_i x^{2i-2} \quad (12)$$

The polynomials must be orthogonal with the condition

$$\int_0^1 W(x^2) P_k(x^2) P_m(x^2) x^2 dx = 0 \quad k \leq m - 1 \quad (13)$$

Choice of the weighting function  $W(x^2)$  completely determines the polynomial, and hence the trial function and the collocation points which are the roots of the Jacobi polynomials.

The coefficients of the Jacobi polynomials for  $w(x^2)=1-x^2$  were given by Villadsen and Stewart [9]. The roots of Jacobi polynomials can be determined by Newton-Raphson method [10]. Also, for various geometries and weighting functions the roots of the Jacobi polynomials can be found in the literature [11,12]. The Jacobi polynomials and the roots for  $N=3$  and  $6$  are shown in Tab. 2 for  $W(x)=1-x^2$ .

N	polynomial	roots
3	$p_3 = 1 - 11x^2 + \frac{143}{5}x^4 - \frac{143}{7}x^6$	0.3631174638 0.6771862795 0.8997579954
6	$p_6 = 1 - 34x^2 + 323x^4 - 1292x^6 + \frac{7429}{3}x^8 - \frac{74290}{33}x^{10} + \frac{111435}{143}x^{12}$	0.2153539554 0.4206380547 0.6062532055 0.7635196900 0.8850820442 0.9652459265

Table 2: Jacobi polynomials and their roots for  $W(x)=1-x^2$  and  $N=3$  and  $6$ .

The gradient and Laplacian operator for the function  $y(x^2)$  of Eq. 12 are expressed at the collocation points:

$$\frac{dy}{dx} = \sum_{i=1}^{N+1} d_i (2i-2)x^{2i-3} \quad (14)$$

$$\nabla^2 y = \sum_{i=1}^{N+1} d_i (2i-2)[(2i-3)+2]x^{2i-4} \quad (15)$$

Now the collocation points are  $N$  interior points  $0 < x_j < 1$  and one boundary point  $x_{N+1} = 1$ . The point  $x=0$  is not included because the symmetry condition requires that the first derivative be zero at  $x=0$  and that condition is already built into the trial function. In matrix notation we have

$$\mathbf{y} = \mathbf{Qd} \quad \frac{d\mathbf{y}}{dx} = \mathbf{Cd} \quad \nabla^2 \mathbf{y} = \mathbf{Dd} \quad (16)$$

Where

$$Q_{ij} = x_j^{2i-2} \quad C_{ij} = (2i-2)x_j^{2i-3} \quad D_{ij} = \nabla^2(x^{2i-2}) \Big|_{x_j} \quad (17)$$

Solving for  $\mathbf{d}$  gives

$$\frac{d\mathbf{y}}{dx} = \mathbf{CQ}^{-1}\mathbf{y} = \mathbf{Ay} \quad \nabla^2 \mathbf{y} = \mathbf{DQ}^{-1}\mathbf{y} = \mathbf{By} \quad (18)$$

$y_j$  is the unknown value of  $y$  at the interpolation point  $x_j$ . When the  $(N+1)$  interpolation points are chosen the matrices  $\mathbf{A}$  and  $\mathbf{B}$  are completely known.

## Results and discussion

To determine the effectiveness factor the diffusion coefficient is required. The diffusion coefficient for transitional diffusion regime can be obtained from following equation for uniform pore size distribution.

$$D_{eff}(r) = \frac{\phi}{\tau} \frac{D_{kn}(r)D_m}{D_{kn}(r) + D_m} \quad (19)$$

Where  $D_{kn}(r)$  and  $D_m$  are Knudsen and molecular diffusion coefficients respectively and are defined as follows:

$$D_{kn}(r) = \frac{1}{3} \nu d_p = \frac{1}{3} d_p \left( \frac{8RT}{\pi M} \right)^{1/2} \quad (20)$$

$$D_m = \frac{1}{3} \nu \lambda_m \quad (21)$$

where

$$\nu = \left( \frac{8RT}{\pi M} \right) \quad (22)$$

$$\lambda_m = \frac{1}{2^{1/2} \pi} \frac{k_B T}{\sigma_k^2 p} \quad (23)$$

The effective surface area for a catalyst that operates with molecular diffusion is very low, but the diffusion coefficient is high. For Knudsen diffusion to happen depending on the physical properties of the diffusing species usually the pores are in the range of micro pores and surface area is very high but the problem is very low diffusion coefficient which prevents the species to reach active sites inside the catalyst pores. The mechanisms of diffusion in catalyst depend on pore size, for large pores the molecular diffusion dominates, but for small pores Knudsen diffusion is the main mechanism. Normally to have optimum diffusivity and surface area in heterogeneous catalytic systems the transitional diffusion regime is better in which both Knudsen and molecular or bulk mechanism exist simultaneously [13].

Fig. 1 presents the transitional diffusion coefficient in terms of average pore size for ethylbenzene.

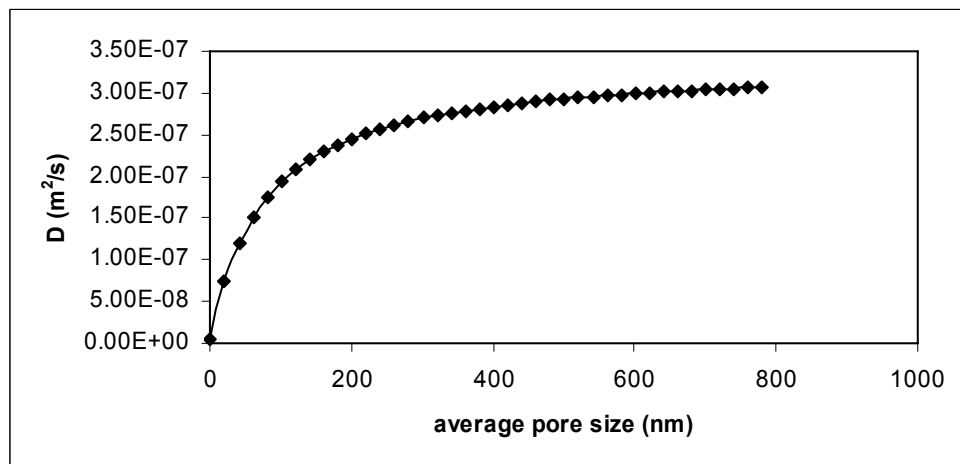


Figure 1. Transitional diffusion coefficient versus average pore size for ethylbenzene at 650° C and atmospheric pressure using average pore size.

In addition the porosity, mean pore connectivity and tortuosity the pore size distribution influences the effective diffusivity. Various unsteady and steady state experimental methods exist to measure the diffusion coefficient precisely [14]. It should be mentioned that measuring the diffusion coefficient at high temperatures has its own technical problems. For sensitivity analysis purposes a quasi experimental method exists to determine the diffusion coefficient using pore size distribution data.

The normal pore size distribution function is presented as follow:

$$f(r) = \frac{1}{\sigma\sqrt{2\pi}} \exp\left(-\frac{1}{2}\left[\frac{r-\mu}{\sigma}\right]^2\right) \quad (24)$$

A real catalyst consists of pores with different sizes; therefore we have a pore size distribution instead of single size pores. Mezedur et al. [15] used ordered and random lattice network modeling to predict the effective diffusivity of reactants and products. Also, the surface effective diffusivity can be estimated by tracer method [16]. Network modeling and tracer method are purely theoretical procedures to determine effective diffusivity. Due to employing experimental pore size distribution data Johanson-Stewart equation gives more realistic results.

Johnson-Stewart equation is:

$$D^* = \int_0^{\infty} D_{eff}(r)f(r)dr \quad (25)$$

Coupling Eqs. 19, 24 and 25 gives a good method to predict the diffusion coefficient at various temperatures and pore sizes. The effective diffusivities of ethylbenzene for various  $\sigma$  (standard deviation) and  $\mu$  (mean pore diameter) were obtained by numerical integration from  $r=0$  to 200 nm using trapezoidal rule and is presented in Fig. 2. The result is for unimodal pore size distribution. A sharp decrease in effective diffusivity can be observed with increasing  $\sigma$  up to 5, after that point the reduction of effective diffusivity is low. It can be seen that in addition to mean pore diameter the type of pore size distribution (flat or narrow) influences the effective diffusivity. Comparison of Figs. 1 and 2 shows that there is a difference between diffusion coefficients obtained by two methods. For example the diffusion coefficient without considering pore size distribution for  $\mu=100$  nm in Fig. 1 is  $1.75 \times 10^{-7}$  m<sup>2</sup>/s. For same mean pore diameter Fig. 2 shows diffusivity ranging from  $2.0 \times 10^{-7}$  to  $3.75 \times 10^{-7}$  m<sup>2</sup>/s for various standard deviations.

Therefore to determine the diffusion coefficient accurately the standard deviation of the pore size distribution curve should be considered.

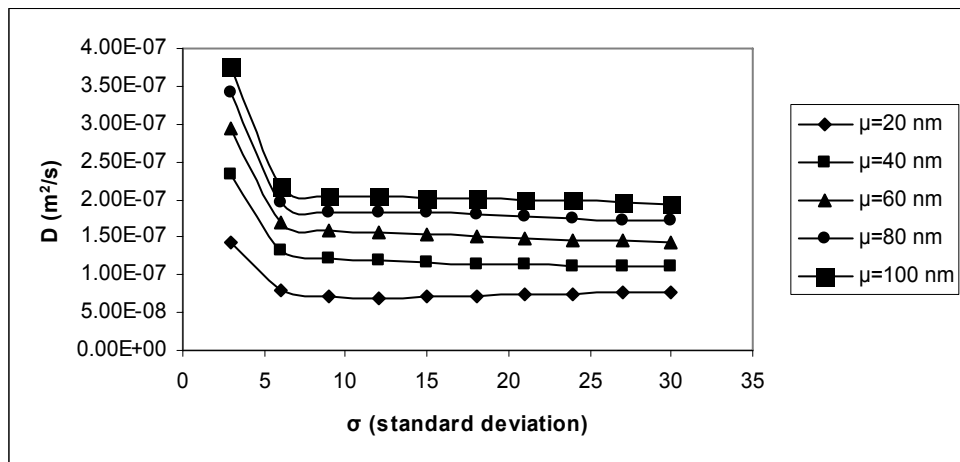


Figure 2. Transitional diffusion coefficient versus  $\sigma$  at various  $\mu$  for normal pore size distribution for ethylbenzene at 650 °C and atmospheric pressure.

Kinetic diameter of substances involved in styrene synthesis is given in Tab. 3.

Substance	Kinetic diameter (°A)
Ethylbenzene	6.2
Styrene	6.0
Benzene	5.9
Ethane	4.4
Methane	3.8
Water	2.65

Table 3. Kinetic diameter of substances.

The diffusion coefficient for six components involved in styrene synthesis are given in Figs. 3 and 4 for various standard deviation in terms of pore size. For large molecules the diffusion coefficient reaches a limiting value at around 300 nm but for small molecules the diffusion coefficient increases with increasing pore size.

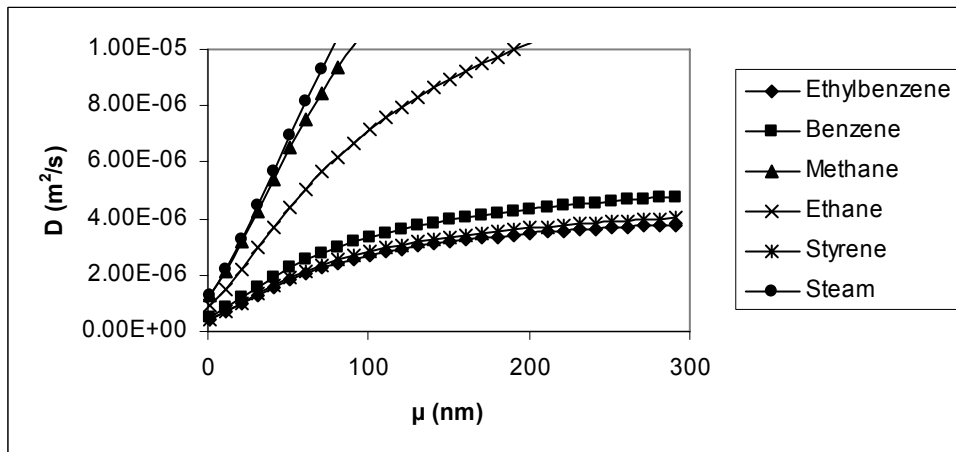


Figure 3. Diffusion coefficient of the components at 650 °C and atmospheric pressure for various  $\mu$  and  $\sigma=15$ .

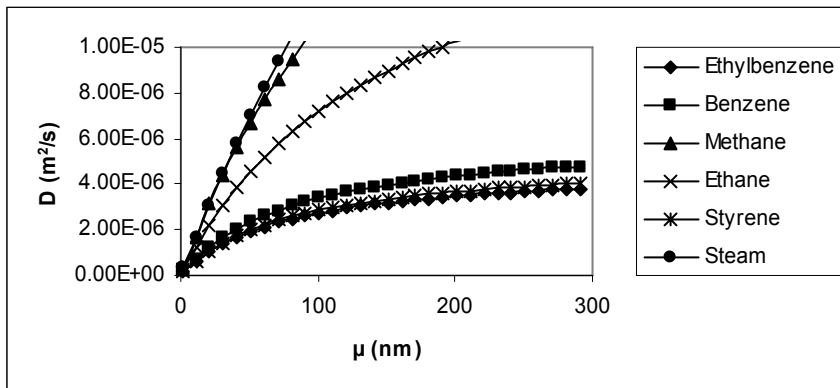


Figure 4. Diffusion coefficient of the components at 650 °C and atmospheric pressure for various  $\mu$  and  $\sigma=3$ .

The point of using bidispersive and bimodal catalyst grains is to upgrade the efficiency of the process. Wide pores facilitate transport of reagents to narrow pores, which, in turn, make their developed surface available to the reagents for the needs of the reaction. The reaction runs in wide and narrow pores. The increase in the radius of the wide pores is concomitant with a decrease in the grain yield, and this indicates that in the wide pores the process runs in kinetic region. Entering the narrow pores, the raw material experiences the resistance of the diffusion which restricts the access of the reagents to the interior of the grain. The efficiency of the catalyst grain depends on the choice of the pore radii, on the ratio of wide pores to narrow pores and on the radius of the grain itself. The bidisperse structure must be optimized with the aim to maximize yield. Prediction of the

effectiveness factor from the conventional monodisperse approach would generally give overestimated values.

Bimodal pore size distribution curve can be obtained by following equation.

$$f_b(r) = \frac{A_\mu}{\sigma_\mu \sqrt{2\pi}} \exp\left(-\frac{1}{2}\left[\frac{r_\mu - \mu_\mu}{\sigma_\mu}\right]^2\right) + \frac{A_M}{\sigma_M \sqrt{2\pi}} \exp\left(-\frac{1}{2}\left[\frac{r_M - \mu_M}{\sigma_M}\right]^2\right) \quad (26)$$

It should be noticed that  $A_\mu$  and  $A_M$  show the number proportions of the micropores to macropores. The volume fraction or the volume occupied by each type of pores at fixed total porosities should be calculated using average pore diameter.

For bimodal distribution with 0 to 20 nm micro pore size distribution and 20 to 100 nm macro pore size distribution considering transitional diffusion the effective diffusivity will be obtained by Wakao-Smith Eq:

$$D_{ws} = \beta_M^2 \int_{20}^{100} D_{eff} f_b(r) dr + \beta_\mu^2 \frac{1+3\beta_M}{1-\beta_M} \int_0^{20} D_{eff} f_b(r) dr \quad (27)$$

The effect of macropore porosity on effective diffusivity of a catalyst with bimodal pore size distribution obtained by numerical integration of Eq. 27 is presented in Fig. 5, assuming total fixed porosity of 0.5 and,  $\sigma_\mu$ ,  $\sigma_M$ ,  $\mu_\mu$ , and  $\mu_M$  equal to, 3, 3, 5 nm, and 70 nm respectively.

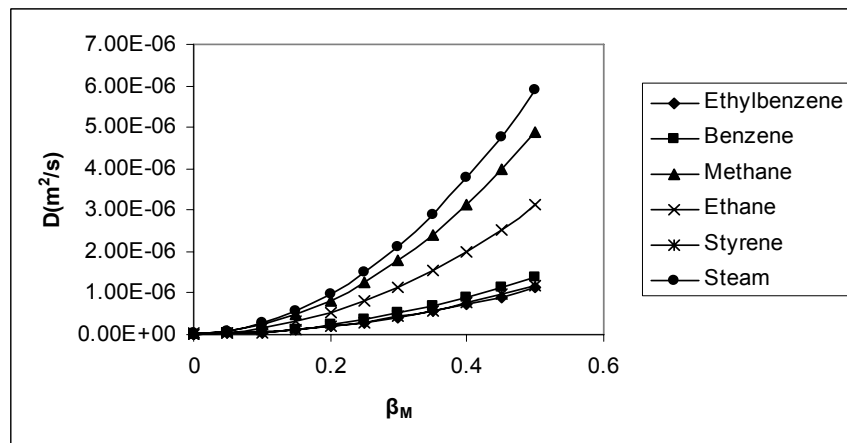


Figure 5. Wakao-Smith transitional diffusion coefficient for bimodal pore size distribution as a function of macropores porosity for various reactants and products.

Fig. 5 shows that bimodal pore size distribution gives  $0.5 \times 10^{-6} \text{ m}^2/\text{s}$  for diffusion coefficient at porosity of macropores equal to 0.35 for average micropore and macropore diameter equal to 5 and 70 nm respectively. Fig. 4 shows that the diffusion coefficient for average pore size of 70 nm in unimodal pore size distribution is equal to  $1.7 \times 10^{-6} \text{ m}^2/\text{s}$ . Comparison of the diffusion coefficients for bimodal and unimodal pore size distribution does not show a considerable difference. It should be considered that including 5 nm pores in bimodal distribution increases the internal surface area significantly. Certainly for other combinations of micropores and macropores better results will be obtained for diffusion coefficient of bimodal pore size distribution.

Using stoichiometric relation the partial pressure of products, hydrogen and styrene in terms of partial pressure of ethylbenzene are presented as follows:

$$p_{H_2}^* = 1 + \frac{p_{EBs} D_{EB}}{p_{H_2s} D_{H_2}} (1 - p_{EB}^*) \quad (28)$$

$$p_{ST}^* = 1 + \frac{p_{EBs} D_{EB}}{p_{STS} D_{ST}} (1 - p_{EB}^*) \quad (29)$$

Inserting the Laplacian using Eq. 15 in continuity equation (Eq. 8) for ethylbenzene gives:

$$\sum_{i=1}^{N+1} B_{ji} p_{EBi}^* - \gamma_{EB} r_{EBj} = 0 \quad j=1, 2, \dots, N \quad (30)$$

$$\gamma_{(EB)} = \frac{d_p^2}{4} \frac{R_g T \rho_s}{D_{EB} p_{EBs}} \quad (31)$$

Eqs. 30 and 31 form a set of  $N$  nonlinear algebraic equations, where  $N$  is the number of interior collocation points. By solving above equations simultaneously the partial pressure of 3 components at 6 interior collocation points are obtained. A MATLAB program was developed to solve above nonlinear algebraic equations using Newton-Raphson method. The details of programming and solution method are not given here.

In these calculations the effectiveness factor is determined at various catalyst pore size distribution or diffusion coefficients. Applying industrial styrene production condition is a good method to estimate the pressure of the substances on the surface of the catalyst pellet at steady state which is necessary for boundary conditions. The pressures of the 3 components at 650 °C are presented in Tab. 3. The total pressure is assumed to be equal

to 1 atm. Steam is used in the styrene production for various reasons; the rest of pressure to reach 1 atmosphere is fulfilled by steam. Other data which are used in this calculation are presented in Tab. 4.

substance	EB	ST	H <sub>2</sub>
Pressure (atm)	0.083	8.3x10 <sup>-4</sup>	4.4x10 <sup>-3</sup>

Table 3. Components pressure on the surface of the catalyst pellet.

Physical property	notation	value
Catalyst pellet density (kg/m3)	$\rho_s$	1250
Catalyst internal void fraction	$\phi$	0.4
Tortuosity factor of the catalyst	$\tau$	3
Catalyst pellet diameter (m)	$d_p$	0.0055

Table 4. Data required for the calculation.

Eq. 30 were solved for 6 interior collocation points. The results for pressure gradients at various  $\gamma_{EB}K1$  are presented in Fig. 6.  $\gamma_{EB}K1$  is presenting the ratio of reaction rate to diffusion rate. As it is seen with increasing  $\gamma_{EB}K1$  which shows decreasing the diffusion rate the slope of the pressure gradient curve increases. There is a good diffusion of the ethylbenzene inside the catalyst pellet at  $\gamma_{EB}K1=1$ , but as it will be explained later this is not a practical range of the ratio of reaction rate to diffusion rate. The pressure gradients for the products, styrene and hydrogen can be obtained by Eqs. 28 and 29.

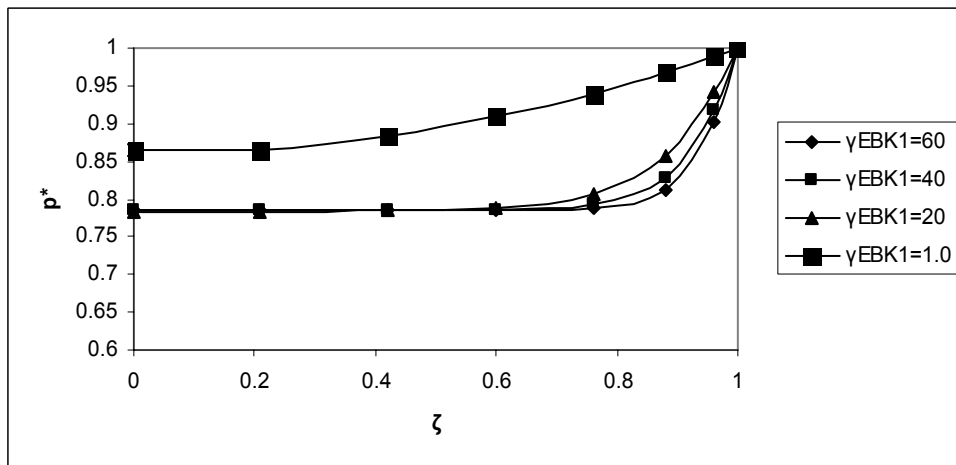


Figure 6: Ethylbenzene pressure gradient inside the catalyst pellet

It is important to compare actual pellet production rate to the rate in the absence of diffusional resistance. If the diffusion were arbitrarily fast, the concentration everywhere in the pellet would be equal to the surface concentration. The effectiveness factor is defined as follows:

$$\eta = \text{effectiveness factor} = \frac{\text{actual reaction rate}}{\text{reaction rate at surface condition}}$$

The effectiveness factor for various pressure gradients can be determined using following equation:

$$\eta = \frac{\sum_{j=1}^{N+1} W_j p^*_j}{\sum_{j=1}^{N+1} W_j} \quad (32)$$

$P^*$  is the solution of equation 21. and  $W$  can be obtained by following matrix equation:

$$\mathbf{W} = \mathbf{f} \mathbf{Q}^{-1} \quad (33)$$

Where the elements of  $\mathbf{f}$  matrix for spherical coordinate are equal:

$$f_i = \frac{1}{2i+1} \quad (34)$$

For endothermic reactions  $\eta$  always is less than unity. Fig. 7 presents the effect of  $\gamma_{EB}K1$  on effectiveness factor. As it is seen a sharp decrease in effectiveness factor can be seen when  $\gamma_{EB}K1$  increases from 1 to 20. From 20 to 60 a moderate decrease observed in the effectiveness factor. After 60 the effectiveness factor almost remains constant. It can be

concluded that decreasing the diffusion rate or increasing the reaction rate does not affect the effectiveness factor after  $\gamma_{EB}K1=60$  for styrene production. The effectiveness factor in terms of  $\gamma_{EB}K1$  is less than unity therefore, almost for the entire practical values of  $\gamma_{EB}K1$  the rate of diffusion controls the overall reaction rate. For  $\gamma_{EB}K1$  less than unity the intrinsic reaction rate controls the overall reaction rate and diffusion rate does not influence the overall reaction rate. In this case to increase the overall reaction rate other parameters such as temperature, pressure, adsorption and desorption of reactants and products and development high efficient new composition catalyst must be considered. For endothermic reaction in an adiabatic reactor  $\eta$  is reducing with the length of the reactor due to reduction of temperature. Also due to temperature gradient development inside the catalyst pellet  $\eta$  is different along the catalyst radius.

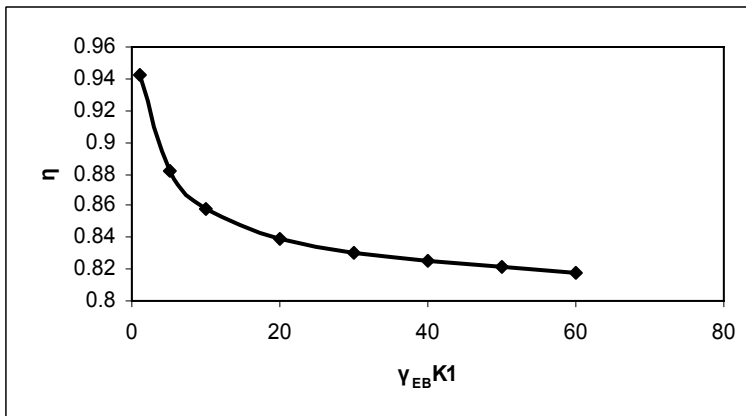


Figure 7: variation of effectiveness factor with  $\gamma_{EB}K1$ .

$$r_{ap} = \eta r_s = \eta K_1 (p_{EBs} - p_{H_2s} p_{STS} / K_{EB}) \quad (35)$$

Catalyst production rate for in terms of  $\eta$  is presented in Fig. 8. It can

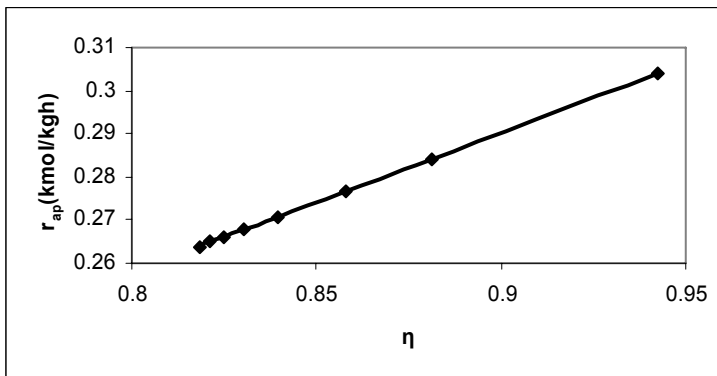


Figure 8: Variation of production rate with effectiveness factor.

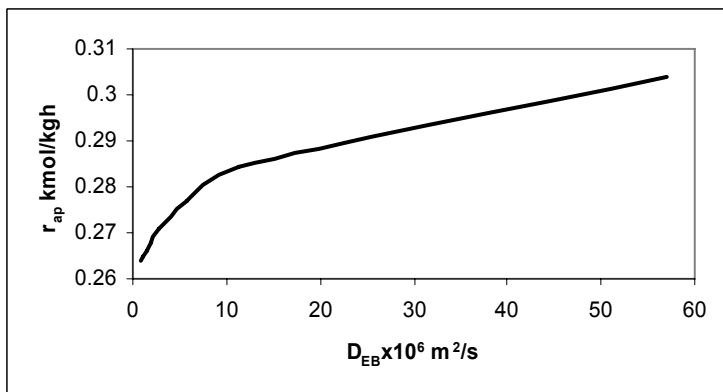


Figure 9: Variation of production rate with diffusion coefficient.

be observed that with increasing the effectiveness factor the production rate increases linearly. Fig. 9 shows the effect of diffusion coefficient on production rate.

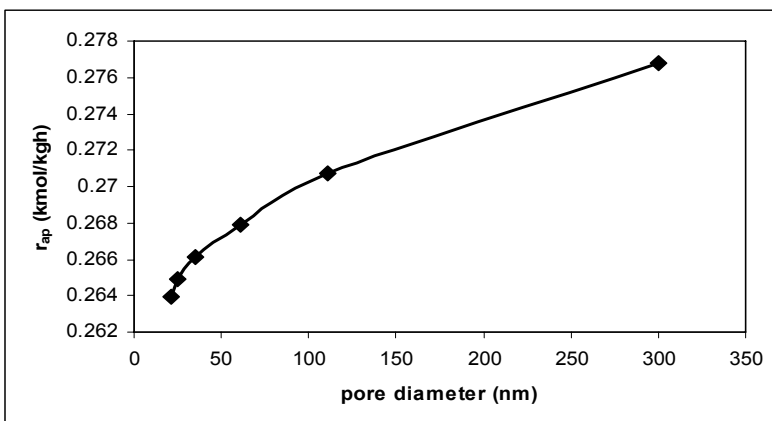


Figure 10: Variation of production rate with average pore diameter

Production rate was determined in terms of pore size using data of Fig. 3 and is presented in Fig. 10. These pore sizes present the highest and lowest achievable diffusion coefficients in practice of catalyst preparation. In actual industrial condition the chemical composition of atmosphere surrounding the catalyst pellet is changing with the reactor length. Precise determination of production rate in an actual reactor needs further investigation but an estimate of the production rate presents that modification of pore size of the catalyst increases the production rate by 0.045.

## **Conclusion**

Diffusion coefficients for single pore, unimodal and bimodal pore size distribution using Stewart-Johnson equation and assuming transitional diffusion regime were determined. There is limiting value for diffusion coefficient when pore size of the catalyst increases. The maximum diffusion coefficient is achieved at around 300 nm average pore size. Determination of diffusion coefficient using average pore size underestimates the diffusion coefficient. The standard deviation or the shape of pore size distribution curve regardless of average pore size influences the diffusion coefficient. With preparation bimodal catalyst pores high diffusion coefficient and internal surface area can be achieved. The effectiveness factor is significantly increasing with increasing the pore size of the catalyst. The limit of pore size for maximum production rate or effectiveness factor is 300 nm. Further increase in pore size does not influence the production rate. Variation of catalyst pore size in practical rage can increase the production rate by 4.5%.

## **Symbols Used**

$A_i$ =frequency factor

$D_{kn}$ =Knudsen diffusion coefficient

$D_m$ =molecular diffusion coefficient

$d_p$ =catalyst pellet diameter

$E_i$ =activation energy

$K_{EB}$ =equilibrium constant

$k_B$ =Boltzman constant

$M$ =molecular weight

$p_m$ =dimensionless pressure

$p_{ms}$ =partial pressure at catalyst pellet surface

$r$ =catalyst pellet radius

$R_g$ =gas constant

$x=x$  coordinate

$y=y$  coordinate

$\rho_s$ =catalyst density

$\zeta$ =dimensionless radius

$\varphi$ =porosity

$\tau$ =tortousity

$\sigma_k$ =kinetic diameter

$\sigma$ =standard deviation

$\mu$ =mean pore diameter

## References

- 1-Lee, E. H., *Catal. Rev.-Sci. Eng.*, 8, 285, (1973) .
- 2-Shekhhah, O. Styrene synthesis In situ characterization and reactivity measurement on un-promoted and potassium promoted iron oxide model catalysts., PhD thesis, Berlin (2004).
- 3-Bin, X., Hengyong X. and Wenzhao L., *Chinese Journal of Catalysis*, 28 (10), 841, (2007).
- 4-William P. Addiego, Wei L., Thorsten, B., *Catalyst Today*, 69, 25-31, (2001).
- 5- Raju Burri D., Choi K., Lee J., Han D., Park S., *Catalyst communications*, 8, 43-48, (2007).
- 6- Reddy B. M., Lee S., Han D., Park S., *Applied Catalysis B: Environmental*, 87, 230-238, (2009).
- 7-Davidson, B. and Shah, M. J., *IBM J*.388-391, (1965).
- 8-Elnashaie S. S. E. H., and Elshishini S. S., Modeling, simulation and optimization of industrial fixed bed catalytic reactors, Gordon and Breach, Amsterdam, (1993).
- 9-Villadsen J. V., and Stewart, W. E., *Chemical Engineering Science*, v. 22, 1483-1501, (1967).
- 10-Rice, R., G, and Do, D. D., Applied mathematics and modeling for chemical engineers, John Wiley & Sons, New York, (1994).
- 11-Lin, L. Numerical simulation of pressure swing adsorption process, Master Thesis, Simon Fraser Univ. (1997).
- 12-Finlayson, B. A., Nonlinear analysis in chemical engineering, McGraw-Hill, New York, (1980).
- 13-Zeynali, M. E., *Defect and Diffusion Forum*, 294, 65, (2009).
- 14- Haynes, H. W., *Catal. Rev.-Sci. Eng.*, **30** (4), 563 (1988).

- 15- Mezedur, M. M., Kaviany, M., and Moore, W., *AIChE*, **48** (1), 15 (2002).
- 16- Zalc, J. M., Reyes, S. C., and Iglesia, E., *Chemical Engineering Science*, **58**, 4605 (2003).